Available online at www.sciencedirect.com
SCIENCE DIRECT
ELSEVIER
Polymer 47 (2006) 3661–3673
polymer
www.elsevier.com/locate/polymer

Ablation and thermal degradation behaviour of a composite based on resol type phenolic resin: Process modeling and experimental

Ahmad Reza Bahramian [a], Mehrdad Kokabi [a,*], Mohammad Hossein Navid Famili [a], Mohammad Hossein Beheshty [b]

[a] *Polymer Engineering Group, Tarbiat Modares University (TMU), P.O. Box 14115-143, Tehran, Iran*
[b] *Iran Polymer and Petrochemical Institute, P.O. Box. 14965/115, Tehran, Iran*

Received 25 December 2005; received in revised form 14 March 2006; accepted 15 March 2006
Available online 3 April 2006

Abstract

During atmospheric re-entry, ballistic or space vehicle is subjected to severe aerodynamic heating and its successful return through the Earth's atmosphere depends largely on the provision that is made for reducing aerodynamic heat transfer to its structure. For this purpose ablative heat shield is normally used which undergoes physical, chemical, and mostly endothermal transformations. These transformations produce new liquid or gas phases which are subsequently injected into the environment.

Mass and energy balance equations have been solved in order to model the ablation and thermal degradation behaviour of an ablative composite. A method to determine and calculate some of the parameters in the ablative equation is proposed from the simultaneous thermal gravity and differential scanning calorimetry analysis techniques.

The objective of this work is to model ablating, charring and thermal degradation behaviour of a heat shield resol-type phenolic resin/asbestos cloth composite in oxyacetylene flame test. This requires solving serious heat transfer equations with moving boundaries. Explicit forward finite difference method (FDM) is used for heat transfer calculation. Moving boundaries are fixed by the Landau transformation. The ablation equation has been solved numerically.

Temperature distribution through the composite thickness, temperature of moving surface, and the rate of moving boundary changes are evaluated. The results are in a good agreement with the experimental data obtained from oxyacetylene flame tests. The model can successfully be used for both material selection and thickness calculation in the design of thermal protection shields.
© 2006 Elsevier Ltd. All rights reserved.

Keywords: Ablation; Thermal degradation; Modelling

1. Introduction

Composite laminated structures are being increasingly used in aeronautical and aerospace construction. They are often subjected to the combinations of lateral pressure and thermal loading. Composite structures have high stiffness, strength and fatigue properties. Degradation of physical properties by various environmental free and force effects such as temperature and pressure load is very important factor in prediction the durability of composite materials [1,2].

Thermal degradation of polymer and composite structures is a complex phenomenon and a great deal of research is performed on this subject [1–7]. The thermal degradation of a composite covers a wide field of important processes such as the development of heat resistant, thermal stabilization, and the characterization of high-temperature composites for aircraft and aerospace usage [3].

Generally, the thermal degradation of a polymeric composite follows more than one mechanism, the existence of various concurrent chemical reactions accompanied by other physical phenomena such as evaporation, melting and ablation introduce further complication for the modeling of the degradation kinetics [4,5].

Ablation is an effective and reliable method largely used in aerospace structures to protect the pay load from the damaging effects of external high temperatures. In the ablation process, the high-heat fluxes are dissipated by the material through a series of endothermic processes. That finally led to the loss and the consumption of the material itself. The working process of an ablative heat shield can be briefly summarized as follows; the convective heat that reaches to the vehicle surface is

* Corresponding author. Tel.: +98 21 8801 1001; fax: +98 21 8800 6544.
E-mail address: mehrir@modares.ac.ir (M. Kokabi).

0032-3861/$ - see front matter © 2006 Elsevier Ltd. All rights reserved.
doi:10.1016/j.polymer.2006.03.049

Nomenclature

A	frequency factor of composite (s^{-1})
A_c	frequency factor for char formation (s^{-1})
A_g	frequency factor for gas formation (s^{-1})
C	heat capacity of the composite ($J\,kg^{-1}\,K^{-1}$)
C_1	heat capacity of the fiber ($J\,kg^{-1}\,K^{-1}$)
C_2	heat capacity of the polymer ($J\,kg^{-1}\,K^{-1}$)
C_3	heat capacity of the coke ($J\,kg^{-1}\,K^{-1}$)
C_g	heat capacity of the gas ($J\,kg^{-1}\,K^{-1}$)
C_p	heat capacity of the air ($J\,kg^{-1}\,K^{-1}$)
C1	primary char
C2	secondary char
d_r	diameter of a reference sample (m)
d_t	diameter of a target sample (m)
E	activation energy of composite thermal degradation ($J\,mol^{-1}$)
E_c	activation energy for char formation ($J\,mol^{-1}$)
E_g	activation energy for gas formation ($J\,mol^{-1}$)
$f(\alpha)$	conversion functional relationship
G	mass rate of gaseous products of composite thermo-decomposition ($kg\,s^{-1}\,m^{-2}$)
G1	primary gas
G2	secondary gas
H	heat convection coefficient ($J\,m^{-2}\,K\,s^{-1}$)
h_1	enthalpy of fibre ($J\,kg^{-1}$)
h_3	enthalpy of char ($J\,kg^{-1}$)
h_g	enthalpy of gas ($J\,kg^{-1}$)
h_p	enthalpy of polymer ($J\,kg^{-1}$)
I	enthalpy of surrounding hot gas ($J\,kg^{-1}$)
I^*	reactive intermediate
J	mass rate of pyrolysis of the matrix ($kg\,m^{-3}\,s^{-1}$)
J_0	intensity of volumetric ablation of a composite ($kg\,m^{-3}\,s^{-1}$)
K	thermal conductivity ($J\,m^{-1}\,s^{-1}\,K^{-1}$)
K_0	zero thermal conductivity ($J\,m^{-1}\,s^{-1}\,K^{-1}$)
K	rate constant (s^{-1})
k_C	rate constant for char formation (s^{-1})
k_g	rate constant for gas formation (s^{-1})
k_p	rate constant for polymer formation (s^{-1})
L_0	the initial thickness of composite (m)
m	weight of sample (kg)
m_0	initial weight of the sample (kg)
m_f	final weight of the sample (kg)
m_p	specific pyrolysis mass flow rate ($kg\,m^{-2}\,s^{-1}$)
M_{wg}	average molecular weight of hot gas
n	degree of thermal degradation reaction
n_K	experimental constant of thermal conductivity
P	composite
p	gas pressure (Pa)
p_0	standard pressure equal to 0.1 MPa
q_0	zero heat flux ($J\,s^{-1}\,m^{-2}$)
q_{bl}	the convective heat flux carried off from the heated surface at the expense of injection into the boundary layer of gaseous products of the thermo-decomposition of the composite ($J\,s^{-1}\,m^{-2}$)
q_e	the convective heat flux carried off from the surrounding into the surface ($J\,s^{-1}\,m^{-2}$)
q_K	the heat flux consumed for warming the composite due to heat conduction ($J\,s^{-1}\,m^{-2}$)
Q_p	internal heat source
q_{rw}	the radiation heat flux carried off from the surface at the expense of own radiation of the surface ($J\,s^{-1}\,m^{-2}$)
q_w	the convective heat flux carried off from the heated surface heated up to temperature T_w into the surrounding ($J\,s^{-1}\,m^{-2}$)
R	universal gas constant ($J\,kg^{-1}\,mol^{-1}\,K^{-1}$)
s_1	char moving boundary (m)
s_2	pyrolysis moving boundary (m)
s_3	back of insulator fixed boundary (m)
s_4	back of substrate fixed boundary (m)
S	surface area of cylindrical sample (m^2)
t	time (s)
T	absolute temperature (K)
T_g	glass transition temperature (K)
T_e	hot gas temperature (K)
T_w	surface temperature (K)
V	volatile
V_{gas}	the mass fraction of the resin transformed to the gas in respect to the mass of composite
X_g	the mass fraction of the resin which may be decomposed in respect to the total mass of resin
y	distance (m)
y_c	yield of charring
α	degree of weight loss
β	heating rate ($K\,s^{-1}$)
λ	local mass fraction of polymer
ΔH_p	heat of ablation ($J\,kg^{-1}$)
ΔT_p	temperature difference between initial and final thermal degradation in TG analysis (K)
ΔT_r	temperature difference between two junction of thermocouples used in reference sample (K)
ΔT_t	temperature difference between two junction of thermocouples used in target sample (K)
Δy	the distance differentiate (m)
δ_B	a thin surface layer of thickness that produces the bubbles (m)
δ_r	distance between two junction of thermocouples used in reference sample (m)
δ_t	distance between two junction of thermocouples used in target sample (m)
ε	emission factor
ϕ	expansion coefficient
ξ	Landau transformation
v_1	volumetric concentration of fibres in the composite

v_2	volumetric concentration of polymer in the composite matrix	γ_{bl}	pyrolysis gas blowing coefficient
v_3	volumetric concentration of coke that forms in the matrix during pyrolysis	ρ	density of the composite (kg m^{-3})
v_4	volumetric concentration of pores in the composite	ρ_g	density of the pyrolysis gas (kg m^{-3})
v_4^0	volumetric of initial porosity of the composite at the initial temperature (293 K)	ρ_1	density of the fibre (kg m^{-3})
Γ	Gasification coefficient of the matrix	ρ_2	density of the polymer (kg m^{-3})
		ρ_3	density of the coke (kg m^{-3})
		σ	Stefan Boltzman constant (J m^{-2} K^{-4})

balanced by surface radiation, phase transitions, and chemical reactions. Moreover, part of the incoming convective heat flux is blocked by the outcoming flow of hot gases that result from the degradative processes. The ablative material keeps the surface temperature within a certain range and as a consequence an increase of the heat flux will not cause a consistent temperature raise, but will cause an increase of the surface recession rate [5,6].

Charring ablators produce char as an effect of the thermal degradation reaction. As the charring ablator is heated, the temperature increases until the surface reaches the degradation temperature and starts to release gaseous products, leaving a porous carbonaceous residue, i.e. char. Char formation has long been recognized as an effective means of improving the fire retardancy of synthetic polymers. To predict the ignition characteristics and heat release rate for a char forming material, one must be able to model the production rate of volatile gases from it [7].

In this work, phenolic resin/asbestos cloth ablative composite as heat shield is analyzed. The main objective of this study is to examine the influence of the experimental conditions in estimating the thermal properties of ablative composite materials. In order to achieve this, experimental data and mathematical model are analyzed and compared. The mathematical model of transient processes of heat and mass transfer in composite and characteristics of non-linear optimization model are proposed and confirmed by experiment.

2. Mathematical model of ablation and thermal degradation

2.1. Mathematical model of ablating composite

Under the experimental conditions (oxyacetylene flame test), complex processes of heat and mass transfer take place in the composite. When the composite is exposed to high temperature and high velocity fluid stream, decomposition of resin begins at a pyrolysis temperature and char layer ablation creates at a higher temperature. The free surface of the composite under the influence of high temperature stream is continuously spilled and depends on the oxygen content in the gases, oxidized. Therefore, three zones are formed (Fig. 1): the virgin material, the pyrolysis zone and the porous char layer [8,9].

In this section, the mathematical model illustrating the thermal decomposition and ablation of the composite material is described. The main assumptions on which the model rests are listed below [7,8]:

(i) No energy is transferred by mass diffusion.
(ii) Movement of liquid is assumed negligible compared to pyrolysis gases.
(iii) Pyrolysis gases may be considered 'ideal gases' but their properties will be kept constant.
(iv) Volatiles formed from the polymer escape from the solid as soon as they are formed.
(v) The instantaneous density of the composite depends on the mass fraction of polymer remaining in the solid and behaviour of thermal degradation of polymeric matrix.
(vi) The specific heat capacity of the composite is a mass-weighted average of the relative mass fractions of polymer, char, and fibre remaining in the composite.
(vii) The change of heat conductivity coefficient of the composite depends on temperature change.
(viii) The decomposition of polymer (weight loss) occurs in a single step and exhibits a first order reaction.

Hence, the problem can be described by the following transient partial differential heat conduction equation [10]

$$\rho C \frac{\mathrm{d}T}{\mathrm{d}t} = \frac{\partial}{\partial y}\left(K\frac{\partial T}{\partial y}\right) + C_g m_p \frac{\partial T}{\partial y} + (h_g - \bar{h})\frac{\partial \rho}{\partial t} \quad (1)$$

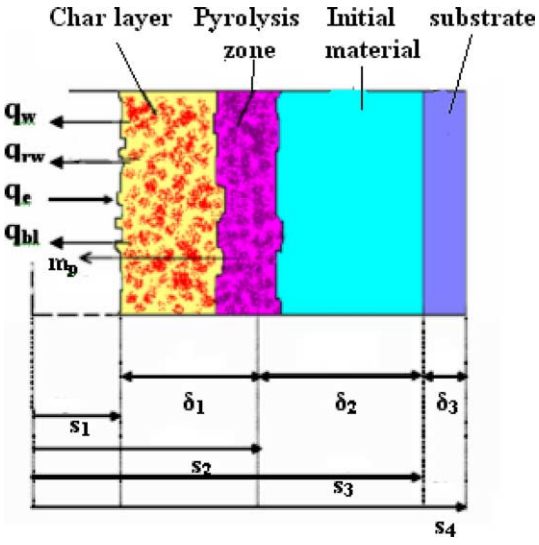

Fig. 1. The zones within the ablating composite [8].

where

$$(h_g - \bar{h}) = \Delta H_p \tag{2}$$

$$(h_g - \bar{h})\frac{\partial \rho}{\partial t} = Q_p(T) \tag{3}$$

$$\bar{h} = \frac{\rho_1 h_1 - \rho_3 h_3}{\rho_1 - \rho_3} \tag{4}$$

In order to solve this equation, it is necessary to calculate and determine thermophysical properties during thermal degradation and ablation. These properties, such as the thermal conductivity, K, specific heat, C, and density, ρ, all change by thermal degradation of composite. The methods required to obtain these parameters will be described in Section 2.2.

The term $(h_g - \bar{h})$ is calculated, using differential scanning calorimeter, DSC. In fact, this parameter represents the heat of ablation obtained by measurement of DSC under curve surface area [10,11].

We solve the ablation equation (Eq. (1)) using a front-fixing method, where the moving front is made stationary by the Landau transformation:

$$\xi = \frac{y - s(t)}{L_0 - s(t)} \tag{5}$$

The ablation equation then becomes:

$$\rho C \frac{\partial T}{\partial t} = \frac{K}{(L_0 - s(t))^2}\frac{\partial^2 T}{\partial \xi^2} + \frac{1}{(L_0 - s(t))^2}\left(\frac{\partial T}{\partial \xi}\right)^2 \frac{\partial K}{\partial T} + \frac{m_p C_g + \rho C\left(\frac{\partial s(t)}{\partial t}\right)(1-\xi)}{(L_0 - s(t))}\frac{\partial T}{\partial \xi} + Q_p(T) \tag{6}$$

The ablation model involves three zones and two moving boundaries, s_1 and, s_2, Fig. (2). Third and fourth boundaries, s_3, and, s_4 are fixed. Corresponding equations for defining boundaries are achieved from mass balance equation as follow (for this purpose the mechanical erosion is assumed negligible) [8,12]:

$$\frac{\partial m}{\partial t} = m_p|_y - m_p|_{y+\Delta y} = m_p|_y - m_p|_y + \frac{\partial}{\partial y}(m_p \Delta y) \tag{7}$$

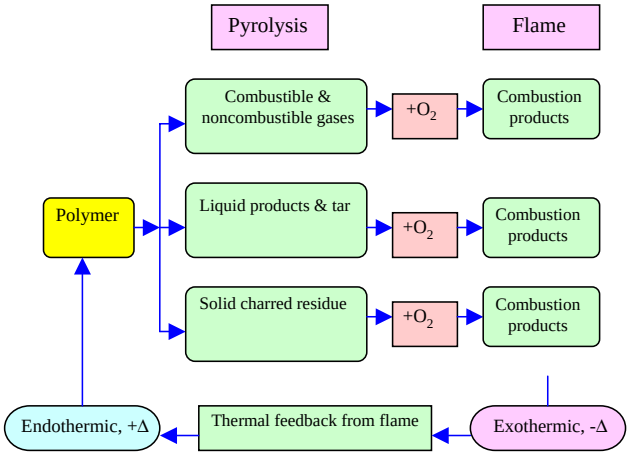

Fig. 2. Thermal degradation process of a solid polymer [17].

$$\Rightarrow \frac{\partial}{\partial t}(\rho \Delta y) = \frac{\partial}{\partial y}(m_p \Delta y)$$

Therefore:

$$m_p = \int_{y_1}^{y_2} \frac{\partial \rho}{\partial t} dy \tag{8}$$

One can rewrite this equation as follows:

$$m_p = \frac{\partial \rho}{\partial t}\frac{\partial s(t)}{\partial t} \tag{9}$$

So:

$$s_2(t) = \int_0^t \frac{m_p}{\rho - \rho_3} dt \tag{10}$$

And a relationship between the top of the char region and the polymer–pyrolysis interface can be found [12]:

$$s_1(t) = s_2(t) + \phi(L_0 - s_2(t)) \tag{11}$$

The boundaries $s_1(t)$ and $s_2(t)$ can be verified by direct measurement of the sample at various stages of degradation which is explained in the experimental section.

$$s_3(t) = \text{const.} \tag{12}$$

$$s_4(t) = \text{const.} \tag{13}$$

where $\phi = y_c(\rho/\rho_3)$ is the expansion coefficient [12]. Calculation of y_c will be described in the kinetic models of polymer thermal decomposition reactions in Section 2.3.

To complete the system of equations of the in-depth ablation model, it is essential to include equations for calculation the pyrolysis mass flow rate, m_p. The motion of the pyrolysis zone is defined by kinetics of the phenolic resin decomposition.

As mentioned earlier, it is assumed that the rate of decomposition (weight loss) is expressed by the first order reaction [8] and the mechanism of polymer degradation is single step:

$$-\frac{\partial[\rho(\nu_2 X_g - V_{gas})]}{\partial t} = k\rho(\nu_2 X_g - V_{gas}) \tag{14}$$

where $(\nu_2 X_g - V_{gas})$ represents the mass of decomposed resin with respect to mass of virgin composite. Using the Arrhenius type reaction rate constant, equations for calculation V_{gas} and m_p are obtained as follows:

$$\frac{\partial V_{gas}}{\partial t} = k(\nu_2 X_g - V_{gas}) = A(\nu_2 X_g - V_{gas})e^{-E/RT} \tag{15}$$

$$m_p(t) = \int_0^{\delta_B} \frac{\partial(\rho V_{gas})}{\partial t} = \int_0^{\delta_B} \rho A(\nu_2 X_g - V_{gas}(y,t))e^{-E/(RT(y,t))} dy \tag{16}$$

In Eq. (16), the following relations were experimentally determined by Kanevce [8] for X_g of resol type phenolic

resin matrix:

$$X_g(T) = -0.21322\times10^{-6}\times T^2 + 0.80560\times10^{-3}\times T - 0.12527 \quad \text{for } T < 1255\ \text{K}$$
$$X_g(T) = 0.55 \quad \text{for } T \geq 1255\ \text{K} \tag{17}$$

For the case of a horizontal specimen exposed to a uniform heat flux from above, production of bubbles is restricted to a thin surface layer of thickness δ_B. The approximate size of δ_B may be estimated by matching the net heat flux at the top surface to the temperature gradient. The result is that [7]:

$$\delta_B \approx \frac{K\Delta T_p}{\varepsilon q_0 + h(T_0 - T_p) + \varepsilon\sigma(T_0^4 - T_p^4)} \tag{18}$$

2.1.1. Initial and boundary conditions

The applied initial conditions for the composite take the general form [13,14]:

$$T(y,t)|_{t=0} = T(y,0) = T_0 \tag{19}$$

The boundary conditions are the general conditions of convective, radiative, and blowing exchange at the free composite surface with the convective heat transfer coefficients tuned to the heat flux conditions (Fig. 2).

$$q_K = q_e - q_{rw} - q_{bL} - q_w \quad \text{at } y = s_1(t) \tag{20}$$

where

$$q_K = -K\frac{\partial T}{\partial y}; \quad q_e = h(T_e - T_0); \quad q_{rw} = \varepsilon\sigma T_w^4;$$

$$q_{bL} = \gamma_{bL} G(I)^{-1}(q_e - q_w); \quad q_w = C_p(I)(T_w - T_0)$$

$$\text{and; } \gamma_{bL} = 0.7\left(\frac{M_{wg}}{16}\right)^{0.55},$$

2.2. Thermophysical properties of thermoset composites

As said before, under the action of high temperatures, the composite properties, such as density, heat conductivity, and specific heat, all change. Therefore, to exact solve the ablation equation (Eq. (1)), it is necessary to consider the behaviour of its properties during thermal degradation and ablation as follows.

2.2.1. Density

On heating a polymeric composite to the pyrolysis temperature of its matrix, density of composite decreases due to intensive gas generation in the matrix. It is assumed that the density of the composite in thermal degradation condition depends on the mass fraction of polymer remaining in the solid, char and porosity created during decomposition. The change in density upon heating is described by the equation [15]:

$$\rho = \sum_{i=1}^{3} \rho_i v_i \tag{21}$$

$$\sum_{i=1}^{3} v_i = 1 - v_4 \tag{22}$$

The porosity (v_4) forms during the thermal degradation. At the initial state before heating they are:

$$v_1 = v_1^0; \quad v_2 = v_2^0; \quad v_3 = 0; \quad v_4 = v_4^0; \quad \text{and;} \tag{23}$$

$$\rho = \rho_0 = \rho_1 v_1 + \rho_2 v_2^0; \tag{24}$$

The volume fraction of fibers, v_1, does not change upon heating and the change in the volumetric concentration of polymer and coke phases are described by the equations [3,16]:

$$\rho_2 \frac{\partial v_2}{\partial t} = -J \tag{25}$$

$$v_3 = (v_2^0 - v_2)(1 - \Gamma)\frac{\rho_2}{\rho_3} \tag{26}$$

The rate of pyrolysis, J, depends on the temperature and gas pressure in the pores and is described by the modified Arrhenius equation [16]:

$$J = J_0\left[1 - \frac{p}{p_0}\exp\left(-\frac{2E}{RT}\right)\right]^{0.5}\exp\left(-\frac{E}{RT}\right) \tag{27}$$

The volumetric ablation of composite is achieved by [16]:

$$J_0 = \frac{A_g}{A_c}\frac{\partial \rho}{\partial t} \tag{28}$$

Gaseous products of pyrolysis in pores of the composite are assumed ideal and perfect gas, therefore [13]:

$$p = R\rho_g T \tag{29}$$

2.2.2. Heat conductivity

The change in heat conductivity coefficient of an orthotropic composite under high temperature is described by the formula [15]

$$K = \frac{K_0}{v_2^0}\left(\frac{T}{T_0}\right)^{0.5}(v_2 + n_K v_3) \tag{30}$$

K is directly determined experimentally by considering a specific value for T. Then n_K can be calculated from Eq. (30).

In Eq. (30), changing of the heat conductivity coefficient connected with a growing heat conductivity of the polymeric matrix at the initial stage of heating before thermal degradation of polymeric matrix ($v_2 = v_2^0;\ v_3 = 0;$), and decreasing the heat conductivity with the formation of porosity (decrease of v_2 and increase of v_3). After completion of the pyrolysis of polymeric matrix ($v_2 = 0$), heat conductivity grows again due to increasing heat conductivity coefficient of the coke.

2.2.3. Specific heat

The specific heat of the composite during heating is described as the average value of the specific heats of its

components [15]. Obviously, the specific heat of the composite and the volume fractions of its components are functions of temperature.

$$C = \frac{\sum_{i=1}^{3} \rho_i C_i v_i}{\sum_{i=1}^{3} \rho_i v_i} \tag{31}$$

In Eq. (31), changing of the specific heat connected with a decreasing specific heat of a composite during thermal degradation of polymeric matrix (decrease of v_2 and increase of v_3). After completion of the pyrolysis of polymeric matrix ($v_2=0$), specific heat fixes constant due to specific heat of the coke.

2.3. Kinetic models of polymer thermal decomposition reactions

The scope of this section is to determine the kinetic parameters of the thermal degradation of an asbestos–phenolic resin composite by using thermo-gravimetric analysis. The knowledge of these parameters is required to calculate the variation of thermophysical properties of the thermoset composite and usage of equations mentioned in Sections 2.1 and 2.2.

The steps of the thermal degradation of a polymer in composite are described in Fig. 2 [17]. Thermal degradation requires three processes: heating of the polymer, thermal decomposition and ignition of the gaseous decomposition products in air [16,17]. The thermal feedback of radiant energy causes thermolytic damage of primary chemical bonds in the polymer molecules.

Pyrolysis gases mix and react with air in the combustion zone above the surface releasing heat and producing carbon dioxide, water and incomplete combustion products such as carbon monoxide. The basic thermal degradation mechanism leading to volatile fuel generation in char forming polymers has been described as a generalized chemical bond scission process consisting of primary and secondary decomposition events. The primary decomposition step is main end or side chain scission of the polymer to form intermediates. The primary char decomposes by dehydrogenation to form the secondary gas and thermally stable secondary char [17].

The thermal decomposition of a polymeric composite is assumed to be series parallel reaction processes which include irreversible thermal degradation reactions as shown in Fig. 3. Eqs. (32)–(36) describe these reactions, and Eqs. (37)–(39) extend the model to include condensed phase oxidation reaction of the reactive intermediate, primary and secondary char [17].

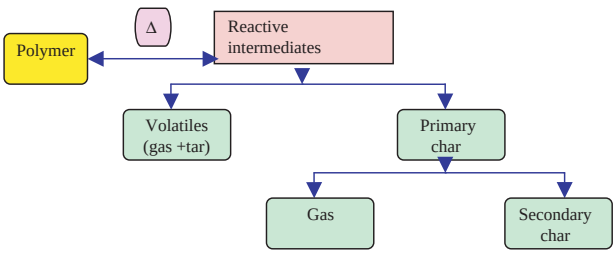

Fig. 3. Primary and secondary decomposition processes in polymer pyrolysis [17].

$$\mathrm{P} \underset{k_{-\mathrm{p}}}{\overset{k_{\mathrm{p}}}{\rightleftarrows}} \mathrm{I}^* \tag{32}$$

$$\mathrm{I}^* \xrightarrow{k_{\mathrm{g1}}} \mathrm{G1} \tag{33}$$

$$\mathrm{I}^* \xrightarrow{k_{\mathrm{c1}}} \mathrm{C1} \tag{34}$$

$$\mathrm{C1} \xrightarrow{k_{\mathrm{g2}}} \mathrm{G2} \tag{35}$$

$$\mathrm{C1} \xrightarrow{k_{\mathrm{c2}}} \mathrm{C2} \tag{36}$$

$$\mathrm{I}^* + \mathrm{O}_2 \xrightarrow{k_{\mathrm{I^*O}}} \mathrm{I^*O_2} \tag{37}$$

$$\mathrm{C1} + \mathrm{O}_2 \xrightarrow{k_{\mathrm{C1O}}} \mathrm{C1O_2} \tag{38}$$

$$\mathrm{C2} + \mathrm{O}_2 \xrightarrow{k_{\mathrm{C2O}}} \mathrm{C2O_2} \tag{39}$$

An analytical solution of the mass loss history of a composite from a kinetic view point is important to understand the thermal degradation process, also creation of combustible gases and char. A simple solution for the mass loss history of a composite allows estimation of the generation rate under isothermal and non-isothermal heating and can be verified using standard laboratory thermo-gravimetric techniques. By considering some assumptions, the process of composite thermal degradation will be reduced and simplified. The following assumptions are considered [17,18]:

(A) The breaking of primary chemical bonds in the polymer is the rate limiting step.
(B) The reactive intermediate is in dynamic equilibrium with the parent polymer.
(C) Thermal degradation of primary char to secondary char and gas is slow compared to the formation of the primary char.
(D) The oxidative environment in the pyrolysis zone of a thermal degradation solid polymer is anaerobic.

Assumptions (A)–(D) led to a simplified mass loss model for polymer combustion as follows [17] (Eq. (32)):

$$\mathrm{I}^* \xrightarrow{k_{\mathrm{g}}} \mathrm{Volatiles} \tag{40}$$

$$\mathrm{I}^* \xrightarrow{k_{\mathrm{c}}} \mathrm{Gases} \tag{41}$$

By using the system of rate equations for the species at time and mass balance equations, we can derive isothermal mass loss equation as follows [17]:

$$\frac{m(t)}{m_0} = 1 - \left[\frac{k_{\mathrm{g}}}{k_{\mathrm{g}} + k_{\mathrm{c}}}\right]\{1 - \exp(-k_{\mathrm{p}} t)\} \tag{42}$$

Eq. (42) shows that as $t \to \infty$ the residual mass approaches an equilibrium value at constant temperature given by [17,14]:

$$\frac{m(\infty)}{m_0} = \left[\frac{k_c}{k_g + k_c}\right] = y_c \tag{43}$$

Assuming Arrhenius forms for k_g, ($k_g = A_g \exp(-E_g/RT)$) and k_c, ($k_c = A_c \exp(-E_c/RT)$) in Eq. (43):

$$y_c = \left[1 + \frac{A}{A_c}\exp\left[\frac{-(E_g - E_c)}{RT}\right]\right]^{-1} \tag{44a}$$

$$\ln\left[\frac{1-y_c}{y_c}\right] = \ln\left[\frac{A_g}{A_c}\right] - \left[\frac{E_g - E_c}{R}\right]\frac{1}{T} \tag{44b}$$

Substituting Eq. (43) into Eq. (42) yields the final results for the isothermal mass loss history in terms of the rate constant for thermolysis of primary chemical bonds in the polymer, k_p:

$$\frac{m(t)}{m_0} = y_c + (1-y_c)\exp(-k_p t) \tag{45}$$

For a constant heating rate, $\beta = dT/dt$, the independent variable in Eq. (45) can be transformed from time to the dimensionless variable. The exact solution of Eq. (45) for the fractional mass as a function of temperature at constant heating rate is [17]:

$$\frac{m(T)}{m_0} = y_c + (1-y_c)\exp\left[-\frac{A}{\beta}(T - T_0)e^{-E_a/RT}\right] \tag{46}$$

The fractional mass loss rate during a linear temperature program is obtained by differentiating Eq. (46) with respect to time. No simple solution is possible when $y_c = y_c(T)$, so we make the approximation that the char yield is constant and independent of temperature, $Y_c = \mu$, and obtain [17]:

$$\frac{-1}{m_0}\frac{dm}{dt} = (1-\mu)k_p(T)\left(1 + \frac{(T-T_0)E_a}{RT^2}\right)\exp\left[\frac{-(T-T_0)k_p(T)}{\beta}\right] \tag{47}$$

For thermo-gravimetric analysis, the degree of weight loss may be defined as the derivative of conversion and particularly as the ratio of actual weight loss to total weight loss corresponding to the degradation process [4–6]:

$$\alpha = \frac{(m_0 - m)}{(m_0 - m_f)} \tag{48}$$

The rate of degradation is dependent on temperature and can be expressed as:

$$\frac{d\alpha}{dt} = kf(\alpha) \tag{49}$$

The temperature dependence of the rate constant may be described by the Arrhenius expression:

$$k = A\exp\left(\frac{-E}{RT}\right) \tag{50}$$

The integrated form of Eq. (49) with respect to temperature and considering the phase boundary reaction method ($f(\alpha) = (1-\alpha)^n$) can be expressed as:

$$F(\alpha) = \int_0^{\infty} \frac{d\alpha}{(1-\alpha)^n} \tag{51}$$

$$\text{For } n = 1: \quad \int_0^{\infty} \frac{d\alpha}{(1-\alpha)^n} = -\ln(1-\alpha)$$

$$\text{For } n \neq 1: \quad \int_0^{\infty} \frac{d\alpha}{(1-\alpha)^n} = \frac{1-(1-\alpha)^{1-n}}{1-n}$$

Therefore, the kinetic model of thermal degradation reactions of polymeric composite has been used to determine all of the kinetic parameters that used to solve ablation equation (Eq. (1)), exactly. The methods required to determine these parameters will be described in the Section 4.

Table 1
Properties of resol type phenolic resin

Property	Unit	Value
Density	kg m^{-3}	1050
Viscosity of liquid resin at 20 °C	Pa s	5.5–6.5
Solid content	wt%	87
Specific heat	J kg^{-1} K^{-1}	2000
Thermal conductivity	J m^{-1} s^{-1} K^{-1}	0.35
Gasification coefficient	–	0.6

3. Experimental

3.1. Materials

A resol type phenolic resin (IL800/2, from Resitan Co.) was used as a polymeric matrix in composite. Properties of this resin are given in Table 1.

Fig. 4 shows the differential scanning calorimetry analysis of the uncured resol type phenolic resin in nitrogen. This curve shows that the precure and cure temperature of phenolic resin are 120 and 160 °C, respectively.

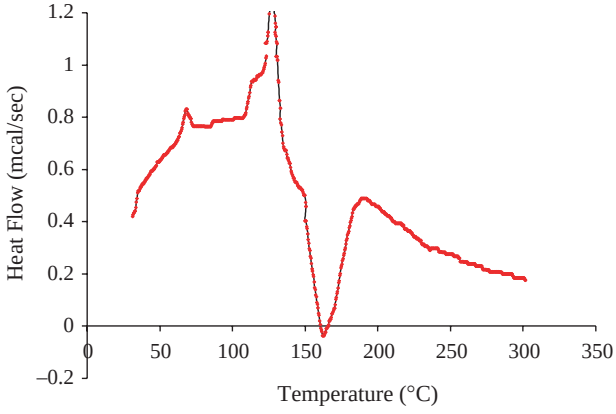

Fig. 4. The differential scanning calorimetry of the uncured resol type phenolic resin in nitrogen.

Table 2
Properties of asbestos cloth

Property	Unit	Value
Density	kg m^{-3}	2000
Specific heat	J kg^{-1} K^{-1}	787
Thermal conductivity	J m^{-1} s^{-1} K^{-1}	0.65
Maximum moisture	wt%	2.5
Minimum asbestos	wt%	90
Maximum mass loss at 820 °C	wt%	23
Weave	–	Plain
Thickness	mm	2

Asbestos cloth (Grade AAA; 1100 g m^{-2}) was added as reinforcing to the polymeric matrix. Properties of asbestos cloth are given in Table 2.

3.2. Preparation of samples

Asbestos cloth impregnated by phenolic resin. Fibre and resin ratio was adjusted to 50/50 wt% (42/58 vol%). The sample was precured at 120 °C for 10 min, and then cured at 160 °C for 1 h in an autoclave. After curing, the composite was post-cured for 0.5 h at 150 °C.

To analyze the temperature at the back of the sample (Back Temperature), a $6\times100\times100$ mm^3 flat sandwich panel structure made of two asbestos cloth layers (4 mm in thickness) and an aluminum substrate (2 mm in thickness) is prepared. For the oxyacetylene flame test and recording the back temperature, the nickel–chrome thermocouple was placed on the back of the sample. This is shown in Fig. 5.

The sample for surface erosion measurement has a cylindrical shape with 10 and 25 mm in diameter and height, respectively. This sample before and after oxyacetylene flame test is shown in Fig. 6. $s_1(t)$ is equal to the height of cylindrical sample after flame test. Therefore, it can be measured, directly. $s_2(t)$ is also an equivalent height of the sample after flame test which is experimentally determined as follows:

$$s_2(t) = \frac{(m_0 - m(t))}{\rho S} \tag{52}$$

The physical and thermophysical properties of asbestos/phenolic composite are given in Table 3.

3.3. Apparatus and procedure

3.3.1. Thermal analysis

Different thermal analysis techniques (TG, TGA) have been used to evaluate the performance of the ablative material and determine the kinetic parameters of thermal degradation. Moreover, differential scanning calorimeter (DSC) has been used to calculate the heat of ablation and specific heat.

Heat weight losses were separately examined by a thermogravimetric analyzer (STA 625, Polymer Laboratories) in air and nitrogen, respectively. Sample size was about 8–10 mg and dynamic experiments were performed at several heating rates:

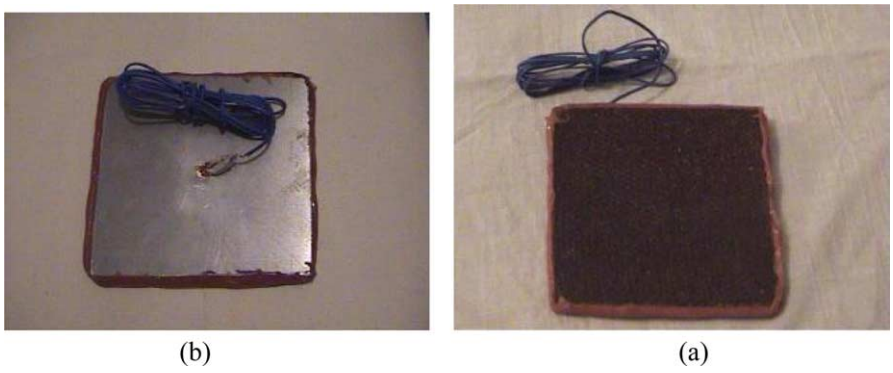

Fig. 5. The sample for oxyacetylene flame test for back temperature analysis, front (a) and back (b) of the sample.

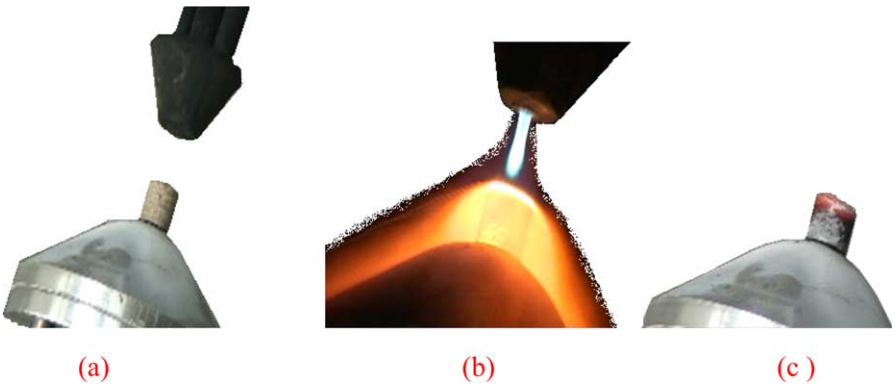

Fig. 6. Measuring the surface erosion by oxyacetylene flame test; before (a), during (b) and after (c) surface erosion test.

Table 3
Physical and thermophysical properties of asbestos/phenolic composite at standard condition

Property	Unit	Value
Density of asbestos/phenolic composite	kg m^{-3}	1450
Density of pyrolysis gas	kg m^{-3}	0.3
Density of char	kg m^{-3}	1089
Specific heat of char	J kg^{-1} K^{-1}	773
Specific heat of asbestos/phenolic composite	J kg^{-1} K^{-1}	1270
Thermal conductivity of asbestos/phenolic composite	J m^{-1}s^{-1} K^{-1}	0.5
Thermal conductivity constant	–	1.5
Volume fraction of phenolic resin	–	0.58
Volume fraction of asbestos fibre	–	0.42

5, 10, 15 and 20 K min^{-1}. Specific heat capacity measurement was done by DSC (PL) at constant heating rate of 10 K min^{-1}.

3.3.2. Thermal conductivity

The thermal conductivity of the composite laminate through its thickness was measured by employing a comparative steady state method against a reference sample according to ASTM E1225-87. At a steady state condition, the thermal conductivity was derived by comparing the temperature gradient between a reference sample and a target one. The thermal conductivity of a target sample, K_t, was calculated using the following equation derived from the Fourier's law of the heat conduction:

$$K_t = K_r \frac{\Delta T_r}{\Delta T_t} \frac{\delta_t}{\delta_r} \frac{d_r^2}{d_t^2} \quad (53)$$

3.3.3. Density

The density and porosity of the composite laminate were determined with submerging in water according to ASTM D-4018.

3.3.4. Specific heat capacity

The specific heat capacity measurements were performed with a differential scanning calorimeter (DSC PL) according to ASTM D-1269. A heating rate of 10 K min^{-1} was used.

3.3.5. Oxyacetylene standard flame test

To evaluate the thermal behaviour and ablation performance of the ablative composite insulators, the oxyacetylene flame test is carried out according to ASTM-E-285-80. This test can be creating hot gas with 3000 K and 8×10^6 W m^{-1} K^{-1} heat flux. Hot combustion gases are directed along the normal to the specimen. The results of the test are useful to show the thermal behaviour of ablative materials. This test method covers the screening of the ablative materials to determine the relative thermal insulation effectiveness when is tested as a flat panel, also the surface erosion when is tested as a cylindrical element in an environment of a steady flow of hot gas provided by an oxyacetylene burner. Fig. 7 shows the oxyacetylene flame test apparatus.

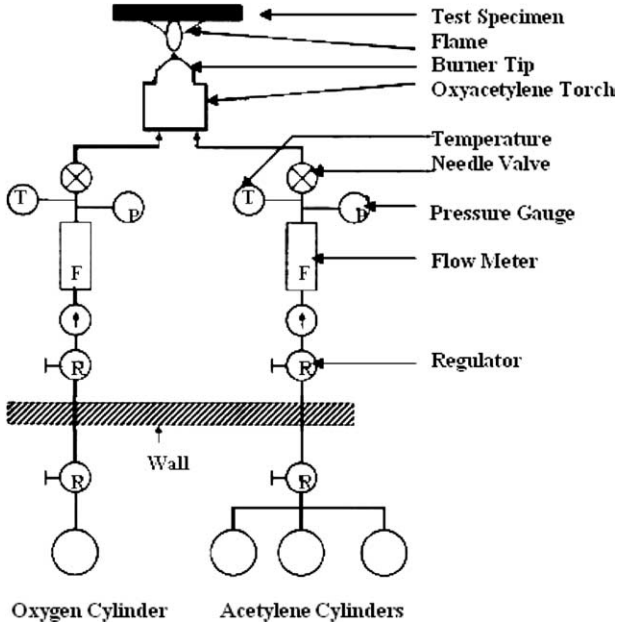

Fig. 7. Standard oxyacetylene flame test apparatus.

4. Results and discussion

The last section of this work is dedicated to the numerical testing of the simulation model. All the experimental data and model equations obtained are now used in an ablation computer program in order to predict the temperature distribution profile through the thickness of the composite ablative material as a function of a given heat flux imposed on its external surface. A finite difference method is used to solve the mass and energy balance equations. While the parameters used in the solution were calculated using the method proposed.

Fig. 8 shows TGA weight loss curves of the phenolic matrix reinforced with asbestos cloth composite at 5, 10, 15 and 20 K min^{-1} in air and nitrogen. The thermal degradation of the composite is single stage, with 50% of residue around 700 K in air and 75% of residue around 1000 K in nitrogen. This curves shows that the entire polymeric matrix removed in presence of oxygen and 50% of polymeric matrix remained in absence of oxygen.

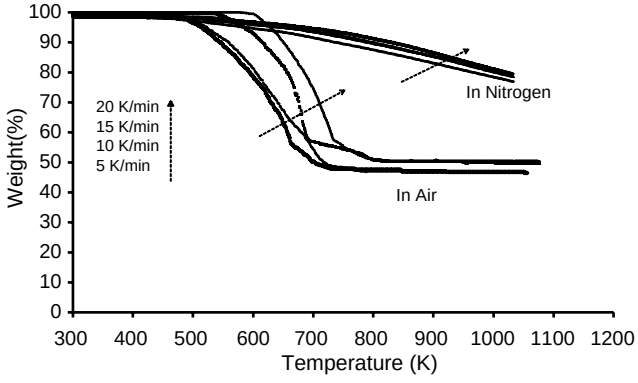

Fig. 8. The thermogravimetric curves of phenolic matrix composite at different heating rates in air and nitrogen.

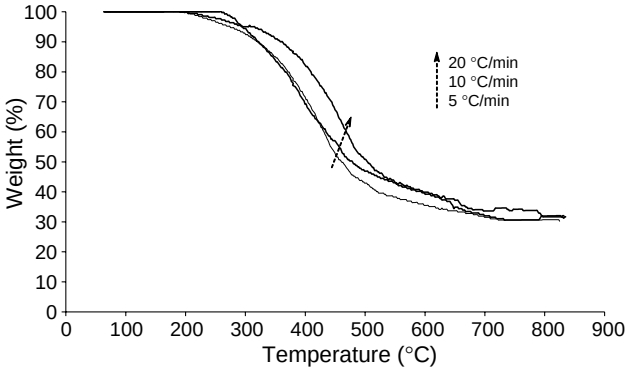

Fig. 9. The thermogravimetric curves of resol type phenolic resin at different heating rates in nitrogen.

Fig. 9 shows TGA weight loss curves of the resol type phenolic resin at 5, 10 and 20 K min^{-1} in nitrogen. The thermal degradation of the resin is single stage, with 30% of residue around 1000 K (700 °C).

The $\ln((d\alpha/dt)/(1-\alpha)^n)$ versus the reciprocal of temperature for asbestos cloth reinforcement composite can be given a linear dependency at correct n. From this correlation, and Eq. (49), the activation energies, E, frequency factor, A, and degree of thermal degradation, n, are evaluated by linear regression analysis of the data points. Fig.10 shows this curve for asbestos cloth/phenolic resin composite in air, too. These curves can be plotted for asbestos cloth reinforcement composite and net resin in nitrogen, alike.

Therefore, the activation energies of composite is 9.57×10^7 J mol^{-1} in air and is 1.75×10^8 J mol^{-1} in nitrogen which is nearly three orders of magnitude larger than the activation energy of neat phenolic resin calculated as 1.43×10^5 J mol^{-1} in nitrogen. This is due to asbestos cloth chemical reactions and its interaction with resin. Similar data were reported by the other researchers (asbestos cloth phenolic resin composite [19], and net phenolic resin [8,20]).

The A, and n for asbestos cloth reinforcement composite are 8.82×10^4 (s^{-1}) and 1.7 in air, and 1.26×10^{10} (s^{-1}) and 6.5 in nitrogen, respectively, and for net phenolic resin in nitrogen are 3×10^9 (s^{-1}) and 1, respectively.

Figs.11 and 12 show TGA weight loss and DSC curves of asbestos/phenolic composite, asbestos cloth, and phenolic resin at 10 K min^{-1} in nitrogen, respectively. In common

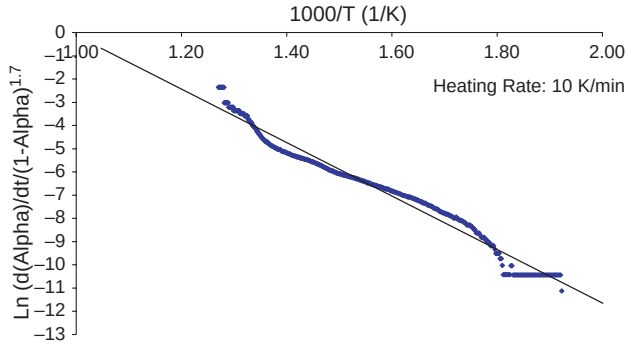

Fig. 10. Plot of the natural logarithm of $(d\alpha/dt)/(1-\alpha)^n$ versus reciprocal temperature of phenolic matrix composite in air.

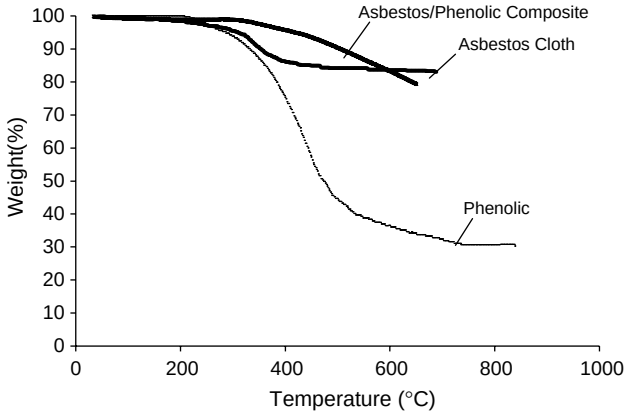

Fig. 11. The thermo gravimetric curves of asbestos/phenolic composite, asbestos cloth, and phenolic resin at 10 °C min^{-1} in nitrogen.

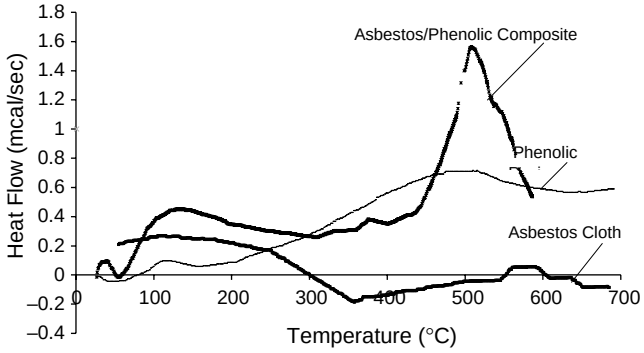

Fig. 12. The DSC curves of asbestos/phenolic composite, asbestos cloth, and phenolic resin at 10 °C min^{-1} in nitrogen.

composites with unreactive reinforcement under 800 °C, such as basalt and high silica fibre, the TGA weight loss curve of composite is between its curve of resin and reinforcement. We can see in Fig. 11 that the thermal resistance of asbestos/phenolic composite is higher than its asbestos cloth and phenolic resin. The residual mass of asbestos cloth, asbestos/phenolic composite, and phenolic resin at 650 °C in nitrogen are 83, 79, and 33%, respectively. Therefore, less than 590 °C, mass loss of asbestos/phenolic composite is lower than mass loss of asbestos cloth and phenolic resin.

Fig. 12 shows that the surface area of endothermic peak (heat of ablation) of composite is greater than the sum of its

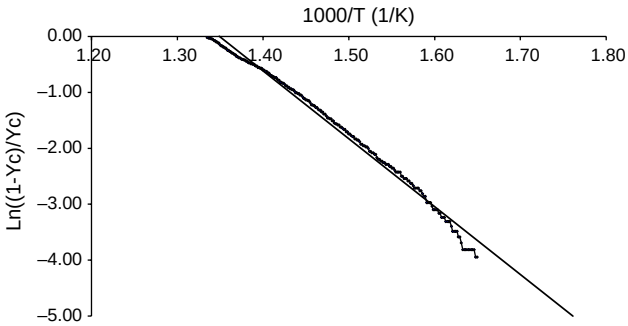

Fig. 13. Plot of the natural logarithm of $(1-Y_c)/Y_c$ versus reciprocal temperature of phenolic matrix composite in air.

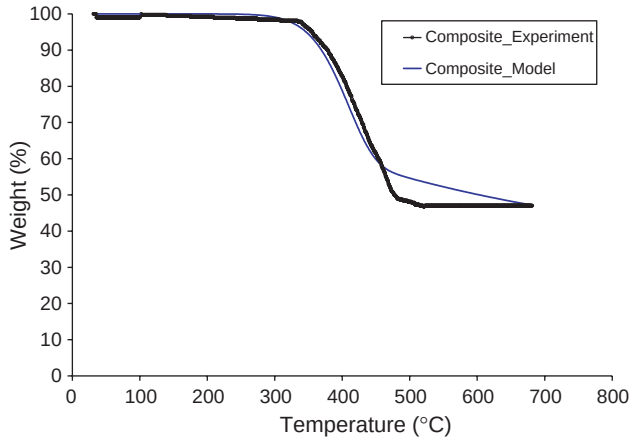

Fig. 14. The thermo gravimetric curves of asbestos/phenolic composite at 10 °C min^{-1} in air, in comparison with model.

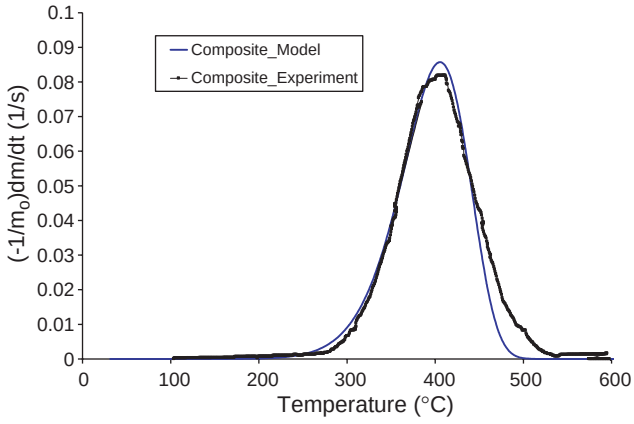

Fig. 15. The differential thermo gravimetric curves of asbestos/phenolic composite at 10 °C min^{-1} in air, in comparison with model.

asbestos cloth and phenolic resin. The reason of this phenomenon is asbestos cloth chemical reactions and its interaction with phenolic resin. Therefore, the activation energy of thermal degradation of asbestos cloth–phenolic resin is more than net phenolic resin.

Table 4
Thermal degradation kinetic parameters of phenolic matrix composite at two environments

Kinetic parameter	Unit	Phenolic resin (in nitrogen)	Composite (in nitrogen)	Composite (in air)
Activation energy E	J mol^{-1}	1.43×10^{5}	1.75×10^{8}	9.57×10^{7}
The difference in activation energy for volatile and char formation, E_g-E_c	J mol^{-1}	4.1×10^{4}	3.92×10^{7}	1.01×10^{7}
Frequency factor, A	s^{-1}	3×10^{9}	1.26×10^{10}	8.82×10^{4}
The fraction of frequency factor for volatile and char formation, A_g/A_c	–	13	46.5	4
Degree of thermal degradation reaction, n	–	1	6.5	1.7

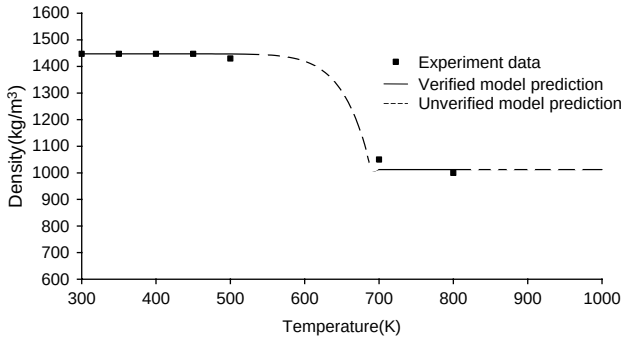

Fig. 16. The variation of density of the phenolic matrix composite versus temperature.

The under curve surface area of DSC curve of asbestos/phenolic composite in Fig.12 is equal to the heat of ablation. Therefore, the heat of ablation of asbestos/phenolic composite is 952 kJ kg^{-1}.

The relative rate constants for volatile and char formation are obtained by plotting Eq. (44b). Thus, a plot of $\ln[(1-y_c)/y_c]$ versus $1/T$ has a slope proportional to the difference in activation energies for volatile and char formation and an intercept which is the natural logarithm of the ratio of the frequencies factors. Fig. 13 shows a plot of Eq. (44b) using the isothermal char yields for asbestos cloth/phenolic resin composite in air. The slope gives $(E_g-E_c)=1.01\times10^{7}$ J mol^{-1} and the intercept, $A_g/A_c=4$. Alike, the (E_g-E_c), and A_g/A_c for asbestos cloth reinforcement composite in

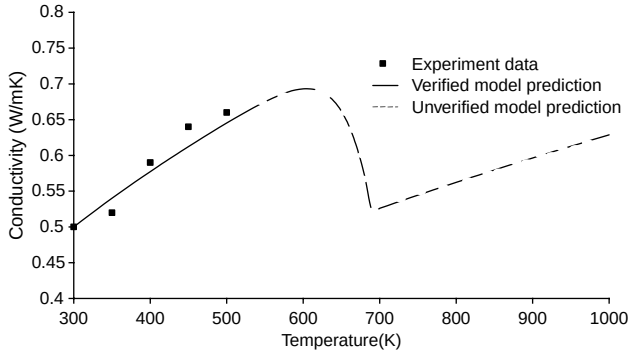

Fig. 17. Non-monotonic character of varying heat conductivity of the phenolic matrix composite.

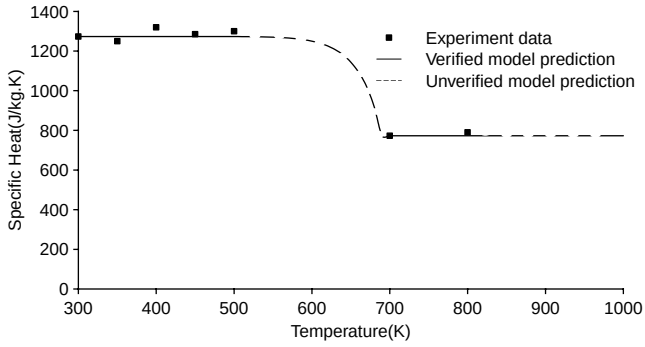

Fig. 18. The change of specific heat of the phenolic matrix composite under heating.

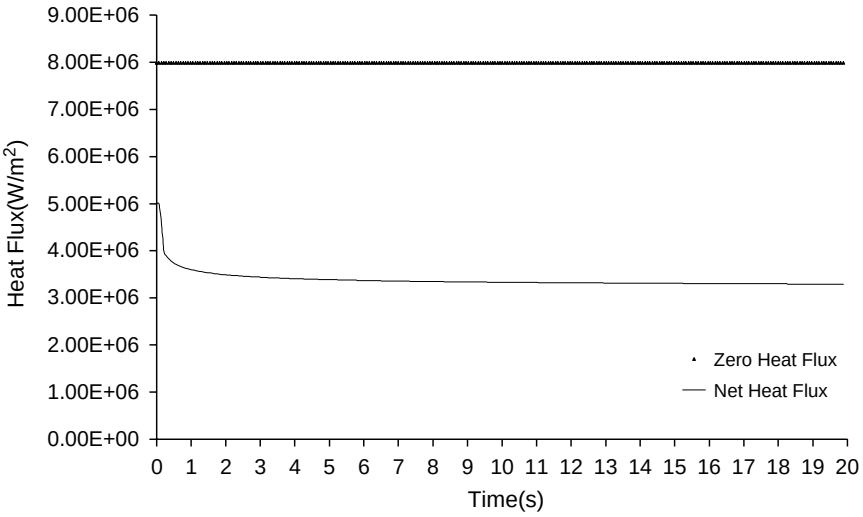

Fig. 19. Zero and net heat flux that applied on surface of asbestos/phenolic composite.

nitrogen are 3.92×10^{7} J mol^{-1} and 46.5, and for net resol type phenolic resin in nitrogen are 4.1×10^{4} J mol^{-1} and 13, respectively.

Figs. 14 and 15 show TGA weight loss and DTA experimental curves of asbestos/phenolic composite at 10 K min^{-1} in air, in comparison with the curves that achieved theoretically by Eqs. (46) and (47), respectively. All of the kinetic parameters were used to plot the TGA and DTA curves, noting to Eqs. (46) and (47). Because of a good agreement between experimental and model curves, as shown in these figures, all of the calculated kinetic parameters are reliable.

All of the kinetic parameters of thermal degradation of phenolic resin and asbestos cloth/phenolic resin are given in Table 4.

Fig. 16 shows the change of density of the phenolic matrix composite under heating. Because of thermal degradation and porosity creation in composite at 500–700 K, density decreases due to decrease in the density of the coke. As seen in this figure the experimental data obtained based on ASTM D-4018 have a good agreement with the theoretical model. Due to polymer thermal decomposition, measurement of the density is impossible.

Fig. 17 shows non-monotonic character of varying heat conductivity of the phenolic matrix composite. Increase in the heat conductivity coefficient at the initial stage of heating is related to the growing heat conductivity of the polymer phase. Upon further heating of the composite to the temperature where pyrolysis begins, the heat conductivity coefficient decreases. This is related to the formation of further porosities in composite. Then, at the end of the pyrolysis and coke formation, heat conductivity coefficient grows again due to the increase in the heat conductivity coefficient of the coke. In Fig. 17, points show the experimental data obtained based on ASTM E1225-87. As observed the experimental has a good agreement with the model under 500 K. According to this standard test method, due to polymer decomposition, measurement of the heat conductivity coefficient upper 500 K is impossible.

Fig.18 shows the change of specific heat of the phenolic matrix composite under heating. The specific heat of the composite was determined as the average value of the specific heat of its components (Eq. (31)). After beginning the thermal degradation and pyrolysis of polymer matrix, the volume fraction of every components of composite are changed that is the cause of the specific heat change. Some experimental data are obtained based on ASTM D-1269. These data have also a good agreement with the theoretical model. Measurement of the specific heat during the composite degradation is impossible due to instantaneous sample mass change.

Fig. 19 shows the zero and net heat flux on composite sample in oxyacetylene flame test. In this test, temperature of flame and convection coefficient is 3000 K and 2960 W m^{-2} K^{-1}, respectively. Therefore, the initial or zero heat flux is equal to 7.99×10^{6} W m^{-2}. During the test time net heat flux decreases because of surface boundary condition (Eq. (20)). Therefore, net heat flux is equal to 3.29×10^{6} W m^{-2} at steady condition. This value is relatively 58.8% lower than zero heat flux.

Fig. 20 shows the char and pyrolysis surface erosion of asbestos/phenolic composite under oxyacetylene flame test condition. After 20 s, the theoretical values of the char and pyrolysis surface erosion are 1.35 and 1.77 mm, respectively.

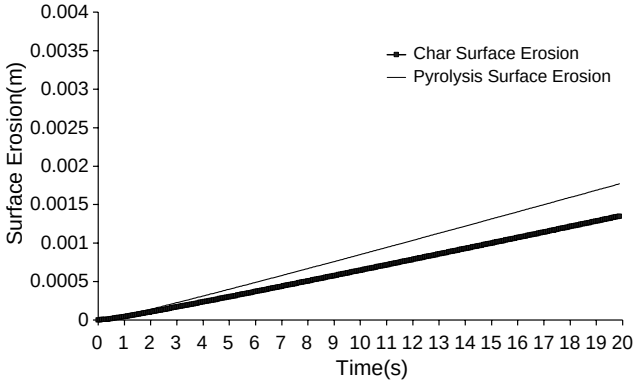

Fig. 20. Char and pyrolysis surface erosion of composite under oxyacetylene flame test condition.

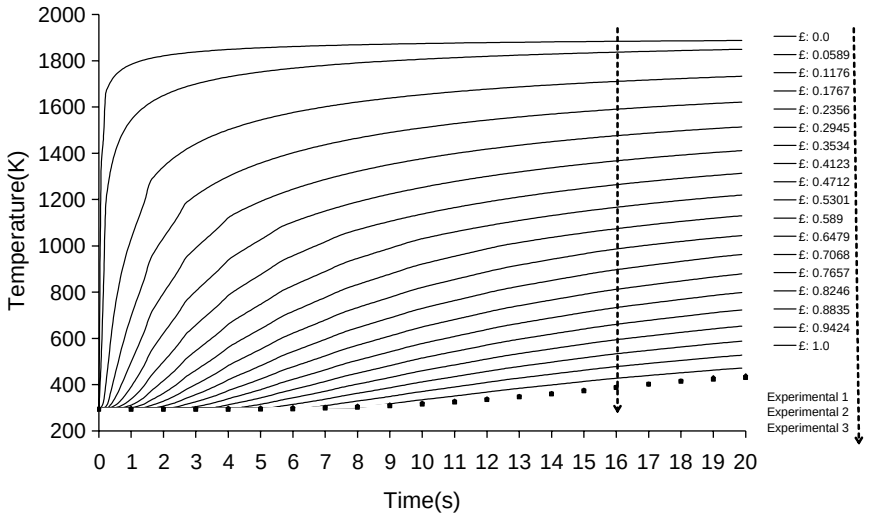

Fig. 21. Temperature distribution through the thickness of asbestos/phenolic composite; dot points are back temperature that measured in oxyacetylene flame test.

The experimental values of these parameters were 1.9 and 2.6 mm, respectively. The most important reason for this difference is the omission of the effect of fluid stream force of oxyacetylene flame in the calculation of the surface erosion (Eqs. (10) and (11)).

Fig. 21 shows the temperature distribution through the thickness of asbestos/phenolic composite based on ablation model prediction. Dot points are back surface temperature that measured experimentally in oxyacetylene flame test. Test time duration is 20 s and front surface temperature rises to 1887 K. After 20 s the model predicts the back surface temperature of a 4 mm thickness asbestos/phenolic composite of 468 K, while oxyacetylene flame tests show these temperatures of 431, 438, and 423 K.

This figure shows a difference between the model and the experimental results. The main reason of this difference is also the omission of the effect of fluid stream force of oxyacetylene flame that causes the mechanical erosion of the surface. Creation of the melting phase from the asbestos cloth and the assumptions in the evaluation of the thermophysical properties with increase of temperature in ablation model could also attribute to this difference.

Despite of simplification of ablation problem, this methodology shows very good reliability in prediction temperature distribution through the thickness of the composite in order to specify its performance under real service conditions.

5. Conclusions

1. A mathematical model describing the peculiarities of the high temperature properties of composites has been developed. The model demonstrates the variation of thermophysical properties such as heat conductivity, density and specific heat at different temperatures.
2. It is also shown that the model is adequately confirmed by the experimental data of the thermophysical and ablation properties of an asbestos/phenolic composite.
3. The mathematical model propounds a simple tool which allows ablation process simulation in design the thickness of a heat shield.
4. In this case study, at conditions of 7.99×10^{6} W m^{-2} external heat flux and 3000 K temperature of hot gas, the back surface temperature and erosion of char surface of a 4 mm thickness asbestos/phenolic composite are equal to 468 K and 1.35 mm, respectively.

References

[1] Shen HS, Zheng JJ, Huang XL. Compos Struct 2003;60:57.
[2] Mouritz AP. J Mater Sci 2002;37:1377.
[3] Kim J, Lee W, Tsai SW. Composites Part B 2002;33:531.
[4] Looyeh 1 MRE, Samanta 2 A, Jihan S, McConnachie J. Int J Numer Meth Eng 2005;63:898.
[5] Torre L, Kenny JM, Maffezzoli AM. J Mater Sci 1998;33:3137.
[6] Cho D, Yoon B. Compos Sci Technol 2001;61:271.
[7] Staggs J. Polym Int 2000;49:1147.
[8] Kanevce LP, Kanevce GH, Angelevski ZZ. Third international conference on inverse problems in engineering, Port Ludlow, WA, USA; 1999. June 13–18.
[9] Mouritz AP. J Mater Sci 2002;37:1377.
[10] Torre L, Kenny JM, Maffezzoli AM. J Mater Sci 1998;33:3145.
[11] Hobbs ML. Polym Degrad Stab 2005;89:353.
[12] Watt SD, Staggs JEJ, McIntosh AC, Brindley J. Fire Saf J 2001;36:421.
[13] Dimitrienko YI, Dimitrienkov ID. Combust Flame 2000;122:211.
[14] Dimitrienko YI. Composites Part A 1999;30:221.
[15] Dimitrienko YI. Composites Part A 1997;28A:453.
[16] Dimitrienko YI. Composites Part A 2000;31:591.
[17] Lyon RE. Polym Degrad Stab 1998;61:201.
[18] Yang MH. Polym Test 2000;19:105.
[19] Determination of kinetic parameters for thermal decomposition of phenolic ablative materials by multiple heating rate method, Naval Surface Weapons Center (N43) Dahlgren 1990; VA 22448.
[20] Chetan MS, Ghadage RS, Rajan R, Gunjikar VG, Ponrathnam S. J Appl Polym Sci 1993;50:685.